



Microwave-assisted catalytic wet peroxide oxidation. Comparison of Fe catalysts supported on activated carbon and γ -alumina

Alicia L. Garcia-Costa ^{*}, Juan A. Zazo, Juan J. Rodriguez, Jose A. Casas

Chemical Engineering, Faculty of Science, Universidad Autonoma de Madrid, Ctra. Colmenar Viejo km. 15, 28049, Madrid, Spain



ARTICLE INFO

Article history:

Received 7 April 2017

Received in revised form 15 June 2017

Accepted 20 June 2017

Available online 8 July 2017

Keywords:

CWPO

Microwave

Fe/AC

Fe/ γ -Al₂O₃

Hot spot

ABSTRACT

This paper studies the role of the catalytic support on microwave-assisted catalytic wet peroxide oxidation (MW-CWPO) with Fe as active phase. Experiments were carried out with and without MW using catalysts of Fe on activated carbon (Fe/AC) and gamma alumina (Fe/ γ -Al₂O₃). Phenol (100 mg L⁻¹) was used as target pollutant, operating at pH 3, 120 °C, 100 mg L⁻¹ catalyst concentration and the theoretical stoichiometric amount of H₂O₂ (500 mg L⁻¹). MW radiation promotes hot spot formation on the surface of AC, enhancing HO_x[•] generation, so that the rate of mineralization is significantly increased with respect to non-assisted CWPO. Under these conditions, phenol oxidation proceeded essentially through direct aromatic ring breakdown, yielding carboxylic acids, while the formation of the highly toxic intermediates hydroquinone and p-benzoquinone were barely detected. The Fe/AC catalyst showed a better performance than the Fe/ γ -Al₂O₃ one, which can be explained by the much higher MW absorption on AC, which, in fact, showed to be a good MW-CWPO catalyst by itself. Meanwhile, the results proved that γ -Al₂O₃ was basically transparent to MW, and deposition of condensation byproducts on the surface hindered the activity of the Fe/ γ -Al₂O₃ catalyst.

© 2017 Elsevier B.V. All rights reserved.

1. Introduction

Environmental policies, with increasingly stringent discharge limits, demand new or enhanced technologies for wastewater treatment, capable to deal with bio-refractory pollutants. Advanced Oxidation Processes (AOPs) have been widely used for this purpose. Among them, Catalytic Wet Peroxide Oxidation (CWPO) is one of the most investigated in the last decade. This AOP uses H₂O₂ as a source of HO_x[•] radicals (HO[•] and HOO[•]) for the abatement of pollutants in water at mild or moderate working conditions (T: 25–120 °C; P: 1–5 bar) [1].

The main points of concern in CWPO are efficient H₂O₂ consumption and catalyst stability. Metals supported on activated carbon (AC) [2–7] or alumina (γ -Al₂O₃) [8–11], or even carbon materials themselves [1,12–15], have been tested for this process. Activated carbon-based catalysts have shown higher activity but lower stability than alumina catalysts, mainly due to active phase leaching [9]. On the other hand, activated carbon by itself gives a lower oxidation rate despite its higher stability [15]. All these cat-

alysts have shown to be highly efficient when working well above ambient-like temperature.

Microwave (MW) radiation has been used for water treatment intensification, since it provides rapid heating and improves energy efficiency [16,17]. MW heating depends on the electric loss tangent ($\tan \delta$), defined as the quotient between ϵ'' , the relative loss factor (which represents the dissipation of the absorbed energy as heat) and ϵ' , the relative dielectric constant (which is the relative measure of the MW energy density in a given material). Thereby, a lossy material with a high ϵ'' is easily heated by MW [17].

$$\tan \delta = \frac{\epsilon''}{\epsilon'} \quad (1)$$

Materials can be classified as opaque, transparent or absorbers, depending on the penetration of MW. Therefore, materials presenting high $\tan \delta$ values are considered MW absorbers, whereas lower values correspond to transparent materials [18].

Table 1 lists those values for different materials. According to them, AC is a MW absorber, whereas Al₂O₃ is transparent to MW. When supporting iron on these materials, $\tan \delta$ increases, being more noticeable this effect for Al₂O₃.

MW-assisted CWPO has been used to treat different synthetic and real wastewaters (Table 2). However, so far there is a lack of reliable and conclusive studies. Even though CuFe₂O₄ and Fe₃O₄ have shown to be effective for Rhodamine B removal in short reac-

* Corresponding author.

E-mail address: alicia.garcia@uam.es (A.L. Garcia-Costa).

Table 1
Dielectric properties of different materials at 25 °C.

Material	tan δ	MW interaction	Reference
PTFE ^a	2.48·10 ⁻⁴	Transparent	[19]
Distilled H ₂ O ^a	0.123	Absorber	[20]
AC ^a	0.57–0.80	Absorber	[21]
AC ^a	0.22–2.95	Absorber	[22]
Carbon nanotubes ^b	1.06	Absorber	[23]
Fe/carbon nanotubes ^b	2	Absorber	[23]
Al ₂ O ₃ ^c	3.10 ⁻⁵ –4.10 ⁻²	Transparent	[24]
Al ₂ O ₃ (99.5%) ^d	8·10 ⁻⁵	Transparent	[25]
Fe/Al ₂ O ₃ ^d	8·10 ⁻⁴	Transparent	[25]

tan δ measured at ^a2,45 GHz, ^b8 GHz, ^c9 GHz, ^d1 GHz.

tion time [26,27], no specific data on mineralization were reported. On the other hand, supported Cu leaches when working in acidic media [35] giving rise to rapid deactivation and turning these catalysts into potential pollutants. Despite using the same active phase [29–31], the role of the support has not yet been analyzed, while it can be a key issue in MW-CWPO. Besides, no studies have been conducted working at high temperature (above 100 °C). Therefore, further research is needed to learn more on the potential application of this technology.

Two well-known catalysts, already used in CWPO of phenol as target pollutant have been tested: (i) Fe on activated carbon (Fe/AC) and (ii) Fe on γ-Al₂O₃ (Fe/γ-Al₂O₃) [2,11]. The aim of this research is to learn on the potential advantage of associating MW radiation to CWPO and analyze the behavior of those two commonly used different supports in the MW-CWPO approach investigated.

2. Materials and methods

2.1. Reagents and materials

Phenol was supplied by Sigma-Aldrich and H₂O₂ (30% w/v) by Panreac. The respective aqueous solutions were prepared at pH 3 using HCl (Panreac). The catalysts were synthesized with Fe(NO₃)₃·9H₂O (98 wt.%) purchased from Sigma-Aldrich and γ-Al₂O₃ and AC supplied by Merck. Working standard solutions of phenol, catechol, resorcinol, hydroquinone, *p*-benzoquinone, and organic acids (fumaric, malonic, maleic, acetic and formic from Sigma-Aldrich and oxalic from Panreac) were prepared for equipment calibration. H₂SO₄ (96 wt.%; Panreac), NaHCO₃ (Merck), Na₂CO₃ (Panreac) and H₃PO₄ (85 wt.%; Sigma-Aldrich) were also used for the analysis. All reagents were of analytical grade and were used as received without further purification. Milli-Q water was always used.

2.2. Catalysts preparation

The preparation of Fe/AC and Fe/γ-Al₂O₃ catalysts was described elsewhere [2,8,11,36]. Briefly, they were prepared by incipient wetness impregnation of AC or γ-Al₂O₃ with an aqueous solution of Fe(NO₃)₃·9H₂O in order to obtain a 4% Fe wt.% nominal

Table 2
Application of MW-assisted CWPO.

	Catalyst	Pollutant	Operating conditions	Results	Ref
Metals	CuFe ₂ O ₄	Rhodamine B (RhB)	T = 80 °C, [RhB] = 100 mg·L ⁻¹ , t = 5 min, P = 300 W	X _{RhB} = 100%	[26]
	Fe ₃ O ₄	Rhodamine B	T = 80 °C, [RhB] = 100 mg·L ⁻¹ , t = 2 min, P = 300 W	X _{RhB} = 99%	[27]
	Iron tailings	Landfill leachate	T = 25 °C, [COD] = 12 g·L ⁻¹ , t = 3 min, P = 480 W	X _{COD} = 45.1%	[28]
Al ₂ O ₃	CuO/Al ₂ O ₃	P-Nitrophenol (NP)	T = 70 °C, [2NP] = 50 mg·L ⁻¹ , t = 6 min, P = 100 W	X _{NP} = 93%	[29]
	CuO/Al ₂ O ₃	2-Nitrophenol	T = 60 °C, [2NP] = 200 mg·L ⁻¹ , t = 5 min, P = 300 W	X _{2NP} = 97%, X _{TOC} = 79%	[30]
	CuO/AC	P-Chlorophenol (PCP)	T = 70 °C, [PCP] = 100 mg·L ⁻¹ , t = 30 min, P = 400 W	X _{TOC} = 90%	[31]
AC	Ferrihydrite/AC	Methyl Orange (MO)	[MO] = 20 mg·L ⁻¹ , t = 4 min, P = 700 W	X _{MO} = 99.1%	[32]
	Cu-Ce/AC	Pharmaceutical wastewater	[TOC] = 158 mg·L ⁻¹ , t = 6 min, P = 539 W	X _{TOC} = 65.9%	[33]
	Fe/AC	Landfill leachate	t = 30 min, P = 720 W	X _{COD} = 93%	[34]

Table 3
Porous texture and Fe content of the supports and catalysts.

	S _{BET} (m ² /g)	A _{ext} (m ² /g)	Fe (%)
AC	1018	175	0.04
Fe/AC	951	73	4.2
γ-Al ₂ O ₃	142	140	–
Fe/γ-Al ₂ O ₃	133	120	4.1

load. Afterwards, the AC-supported catalyst was calcined at 200 °C for 2 h, while for the γ-Al₂O₃ 300 °C and 4 h were used. Under those conditions, Fe₂O₃ was the main iron species in both catalysts.

2.3. Catalyst characterization

The porous texture of the supports and catalysts was characterized by 77 KN₂ adsorption/desorption using a Micromeritics Tristar apparatus. The specific surface area (S_{BET}) and the external or non-microporous area (A_{ext}) were calculated by the BET method and t-method, respectively. The total iron content of the catalyst was determined by inductively coupled plasma mass spectrometry (ICP-MS) using an ICP-MS Elan 6000 Perkin-Elmer Sciex instrument. Additional characterization of these catalysts can be found elsewhere [2,9].

2.4. CWPO and MW-CWPO experiments

All the experiments were carried out at 120 °C and pH₀ = 3 with 100 mg·L⁻¹ of aqueous phenol solution and 100 mg·L⁻¹ of catalyst (particle size < 100 μm). H₂O₂ was added at 500 mg·L⁻¹, corresponding to the theoretical stoichiometric amount for complete mineralization of phenol. Stirring was fixed at 400 rpm, which allowed maintaining the catalyst in suspension and avoiding mass-transfer limitations. All the experiments were done by triplicate, being the standard deviation always less than 5%.

CWPO tests were carried out for 1 h in a batch stainless steel pressurized reactor (BR-300, Berghof) with a 500 mL PTFE insert reaction vessel equipped with backpressure and temperature controllers. When the temperature was equilibrated at 120 °C, hydrogen peroxide solution was injected.

MW-CWPO runs were performed in high pressure 100 mL PTFE reaction vessels in a microwave oven (FlexiWAVE, Milestone) equipped with temperature controller. The reactors were initially loaded with phenol, H₂O₂ and the catalyst and the heating rate was set at 80 °C/min (P_{max}: 1800 W) to reach the reaction temperature (120 °C), which was maintained for 1 h. During reaction, the system pressure rose up to 2.4 bar.

2.5. Analytical methods

Samples were periodically withdrawn from the reactors and immediately analyzed after filtration through fiber glass filters (Albet FV-C). Phenol and aromatic intermediates were identified and quantified by means of an Ultra HPLC (Thermo Scientific Ulti-

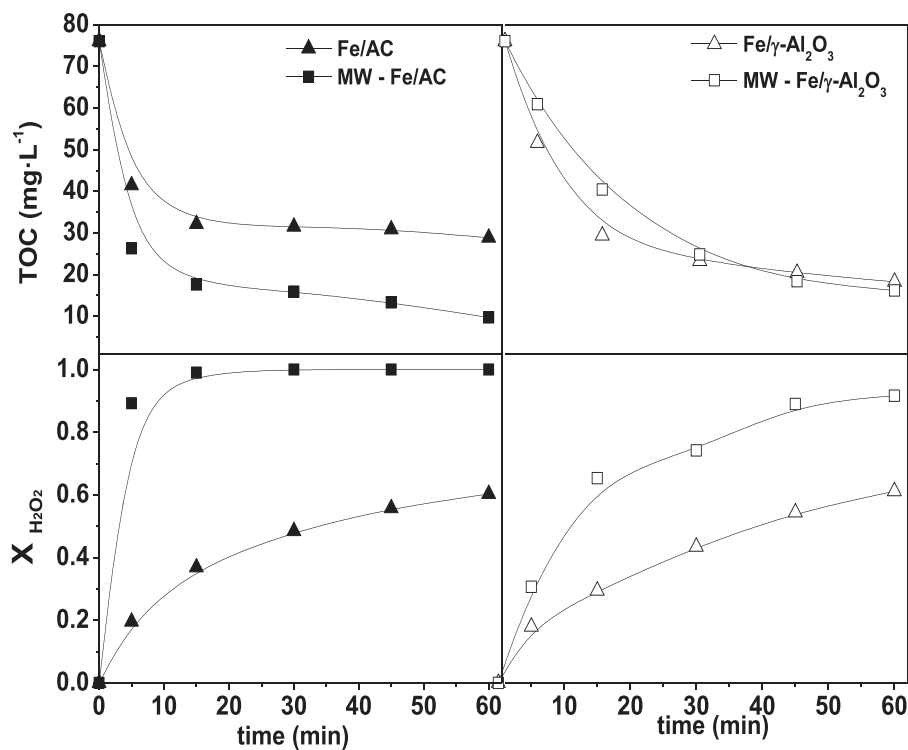


Fig. 1. TOC and H_2O_2 evolution upon CWPO of phenol with and without MW radiation with the catalysts tested. ($[\text{Ph}]_0$: $100 \text{ mg}\cdot\text{L}^{-1}$; $[\text{H}_2\text{O}_2]_0$: $500 \text{ mg}\cdot\text{L}^{-1}$; [cat]: $100 \text{ mg}\cdot\text{L}^{-1}$; T: 120°C and pH_0 : 3).

mate 3000) with a Diode Array detector (Dionex Ultimate 3000). A C18 column (ZORBAX Eclipse Plus C18, 100 mm, $1.8 \mu\text{m}$) was used as stationary phase and a $4 \text{ mM H}_2\text{SO}_4$ aqueous solution at 1 mL/min as mobile phase. UV detector at 210 nm wavelength was used for phenol, resorcinol, catechol and hydroquinone and at 246 nm for *p*-benzoquinone. Short-chain organic acids were analyzed in an ion chromatograph with chemical suppression (Metrohm 790 IC) using a conductivity detector. A Metrosep A supp 5–250 column (25 cm long, 4 mm diameter) was used as stationary phase and 0.7 mL/min of a 3.2 mM/1 mM aqueous solution of Na_2CO_3 and NaHCO_3 , respectively, as mobile phase. Total Organic Carbon was measured using a TOC analyzer (Shimadzu TOC-VSC). Residual H_2O_2 in the liquid phase was determined by colorimetric titration with an Agilent spectrophotometer using the TiOSO_4 method [37].

3. Results and discussion

Table 3 summarizes the BET and external area of the supports and catalysts. AC and Fe/AC have a high developed porosity, corresponding mainly to microporosity, whereas fresh alumina and its catalyst are essentially mesoporous solids with much lower values of surface area. AC has a high adsorption capacity, related to the surface area. Thus, phenol adsorption should be considered. In this

terms, previous to the oxidation runs, blank runs were carried out with the catalysts and phenol (no H_2O_2 added to the solution). TOC did not vary when using either Fe/AC or Fe/γ-Al₂O₃ at 120°C , thus, phenol adsorption is unlikely to occur in the tested conditions. The iron content was around 4 wt.% for the home-made catalysts.

A set of experiments were carried out with and without MW to learn on the effect of this energy source on CWPO. The results are shown in Fig. 1, where it can be seen that MW affects quite differently to the activity of the catalysts tested. In the case of Fe/AC, mineralization was significantly improved, consistently with the enhanced H_2O_2 decomposition rate. This effect is attributed to hot spot formation on the surface of AC. Meanwhile, when using Fe/γ-Al₂O₃, the rate of H_2O_2 decomposition was also increased but in a lower extent and the effect of MW on the CWPO process was irrelevant in terms of mineralization.

The normalized H_2O_2 yield ε , defined as the amount of TOC removed per unit weight of H_2O_2 fed in relation to the maximum theoretical TOC removal at that H_2O_2 dosage, has been used to evaluate the efficiency of H_2O_2 [38]. MW heating allowed increasing this value from 0.77 to 0.88 after 60 min with Fe/AC, whereas with Fe/γ-Al₂O₃, ε remained practically unchanged ($\varepsilon \approx 0.82$). Therefore, H_2O_2 was somewhat more efficient in CWPO with the Fe/γ-Al₂O₃ catalyst, whereas in the MW-assisted process, the AC-supported catalyst showed a significantly improved behavior.

Table 4

Byproducts distribution from MW-assisted and non-assisted CWPO of phenol with the catalyst tested.

Time (min)	CWPO Fe/AC		MW-CWPO Fe/AC		CWPO Fe/γ-Al ₂ O ₃		MW-CWPO Fe/γ-Al ₂ O ₃	
	Acids %	Arom %	Acids %	Arom %	Acids %	Arom %	Acids %	Arom %
5	86.6	13.4	99.5	0.5	63.6	36.4	42.2	57.8
15	98.6	1.4	99.8	0.2	74.6	25.4	63.4	36.6
30	98.5	1.5	100	0	78.3	21.7	77.2	22.8
45	98.4	1.6	100	0	91.3	8.7	89.7	10.3
60	98.2	1.8	100	0	97.2	2.7	94.8	5.2

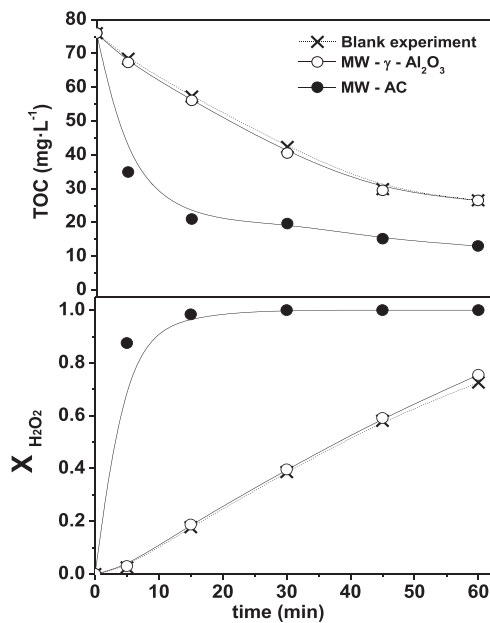


Fig. 2. TOC and H_2O_2 evolution in MW-CWPO of phenol with the bare supports tested and blank experiment with no catalyst. Operating conditions: $[\text{Ph}]_0$: $100 \text{ mg}\cdot\text{L}^{-1}$; $[\text{H}_2\text{O}_2]_0$: $500 \text{ mg}\cdot\text{L}^{-1}$; $[\text{cat}]$: $100 \text{ mg}\cdot\text{L}^{-1}$; T : 120°C and pH_0 : 3.

Table 5
Byproducts distribution from MW-CWPO of phenol with the bare supports.

Time (min)	MW AC		MW $\gamma\text{-Al}_2\text{O}_3$	
	Acids %	Arom. %	Acids %	Arom. %
5	70.5	29.5	29.8	70.2
15	90.6	9.4	23.7	76.3
30	100	0	54.5	45.5
45	100	0	82.6	17.4
60	100	0	91.1	8.9

The distribution of intermediates was followed by means of Ion Chromatography to quantify short chain organic acids, such as acetic, formic, malonic, maleic and oxalic and Ultra HPLC to analyze aromatic compounds, being only detected catechol and *p*-benzoquinone. Byproducts distribution as short chain organic acids and aromatic compounds is shown in Table 4. These results correspond in all cases to complete conversion of phenol, since it was always achieved in less than 5 min.

Under MW-CWPO with the Fe/AC catalyst, phenol disappearance proceeded at a high rate and after 15 min only organic acids were detected, while in the non-assisted process some remaining amounts of aromatic byproducts were still detected even after 1 h reaction time. The highly toxic benzoquinone is of particular concern and in that respect the beneficial effect of MW was very important. With the Fe/ $\gamma\text{-Al}_2\text{O}_3$ catalyst, the residual amounts of aromatic byproducts after 1 h reaction time were still quite significant, being that even more pronounced in the MW-assisted CWPO. To learn more on the specific effect of the support, MW-CWPO experiments with the bare AC and $\gamma\text{-Al}_2\text{O}_3$ were carried out under the same conditions than the previous ones performed with the Fe catalysts. The results are depicted in Fig. 2 in terms of mineralization and H_2O_2 conversion. The evolution of reaction byproducts is given in Table 5, where it can be seen the dramatically different behavior of both supports. The lossy character of AC allows a high MW absorption giving rise to the formation of hot spots on its surface [17,39,40], enhancing wet peroxide oxidation. This phenomenon does not take place, or represents a much less significant contribution, in the case of Fe/ $\gamma\text{-Al}_2\text{O}_3$ since it is a MW insulator,

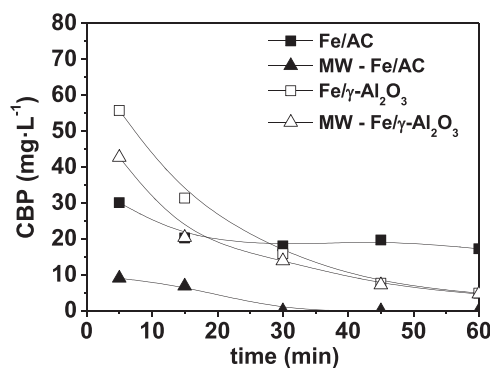


Fig. 3. Condensation byproducts (CBP) upon CWPO with and without MW with the catalysts tested.

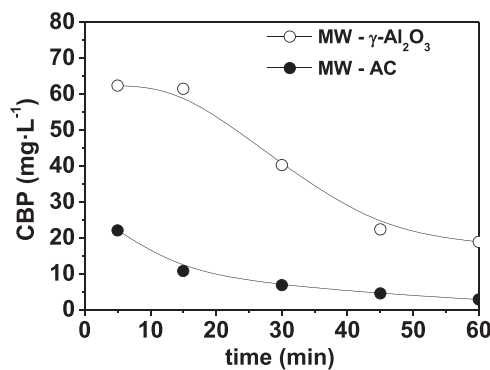


Fig. 4. Condensation byproducts (CBP) upon MW-CWPO with the bare supports.

essentially transparent to MW radiation. Fig. 2 includes the results of a blank experiment performed under MW radiation and the same amount of H_2O_2 , but without any catalyst or support. As can be seen, the $\gamma\text{-Al}_2\text{O}_3$ support does not provoke any significant enhancement on the MW-assisted wet peroxide oxidation. Comparing Fig. 1 and Fig. 2, it can be observed that the dielectric properties of the support play a key role on MW-CWPO. When working with AC as support under MW, iron has a minor contribution in the reaction, since hot spot formation upon the AC surface greatly enhances HO_x^\bullet generation. On the other hand, when working with a MW-transparent support such as Al_2O_3 , the activity of Fe/ Al_2O_3 relies exclusively on the active phase.

It was observed a more or less pronounced difference between the measured TOC and the amount of C associated to the identified species, as can be seen in Figs. 3 and 4 for the catalysts and bare supports, respectively. That difference has been ascribed to oligomeric condensation byproducts (CBP), whose formation has been reported in homogeneous Fenton [41] as well as in CWPO of phenol [1,2,15,42,43]. This refers to CBP in the liquid phase, but those species can be also deposited on the surface of the catalysts. In the case of $\gamma\text{-Al}_2\text{O}_3$ this was confirmed by the dark brown color observed in the solid after use (Fig. 1 of Supporting Information). This darkening of the catalyst was evidenced since the earlier stages of reaction. As can be seen in Fig. 3, the amount of unidentified organic carbon in the liquid phase was significantly higher with the Fe/ $\gamma\text{-Al}_2\text{O}_3$ catalyst and became almost negligible in the MW-assisted CWPO with the Fe/AC catalyst after 30 min reaction time. Fig. 3 also reveals the influence of MW on CBP stability. Hot spot formation on the surface of Fe/AC lead to a complete CBP removal, whereas for Fe/ Al_2O_3 , MW radiation had no effect on the fate of CBP, which are adsorbed on its surface. The results with the bare supports (Fig. 4), show the significantly better performance of AC in that respect.

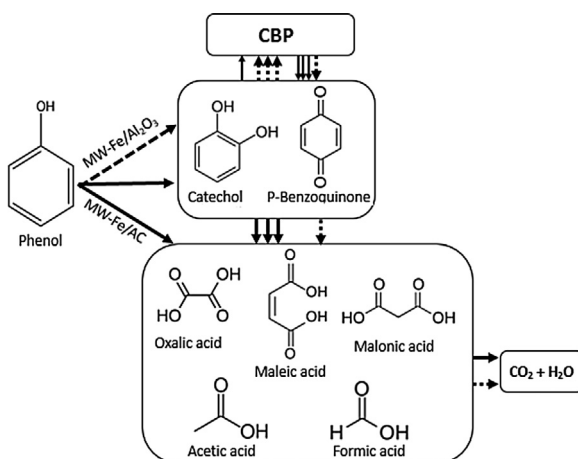


Fig. 5. Reaction pathway of MW-CWPO of phenol with the tested catalysts.

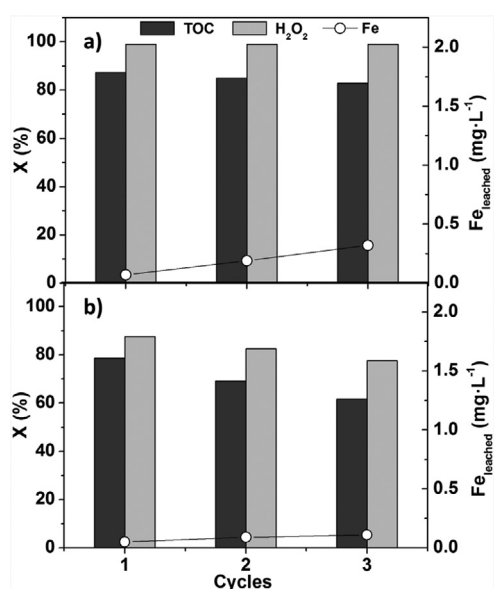


Fig. 6. Stability of a) Fe/AC and b) Fe/Al₂O₃ in MW-CWPO through three reaction cycles. ([Ph₀]: 100 mg·L⁻¹; [H₂O₂]₀: 500 mg·L⁻¹; [cat]: 100 mg·L⁻¹; T: 120 °C and pH₀: 3).

With the results obtained so far, the oxidation route depicted in Fig. 5 is proposed for MW-CWPO of phenol. Starting with phenol, the reaction byproducts are divided in three blocks: aromatic intermediates, short chain organic acids and condensation byproducts. This scheme is consistent with the well-known breakdown routes proposed for Fenton-like oxidation of phenol in the literature [2,41]. As indicated before, with MW-Fe/AC there is a much less formation of CBP, whereas with Fe/γ-Al₂O₃ those species appear in significant amounts since the earlier stages of the process.

Stability of Fe/AC and Fe/Al₂O₃ under MW-CWPO was tested in 3 consecutive cycles. Results are shown in Fig. 6. Fe/AC remained active under the selected operating conditions, since it allowed complete H₂O₂ decomposition in all runs and mineralization degree was always above 80%. Iron leaching was measured after each run. There was a progressive iron leaching ascribed to the action of oxalic acid. Nevertheless, this active phase loss was always below 10%, being this amount negligible regarding homogeneous Fenton contribution. On the other hand, Fe/Al₂O₃ presented a deeply pronounced deactivation due to CBP deposition on the surface of the catalyst, which lead to active sites blockage, hindering

the efficiency of the process for the decomposition of H₂O₂ as well as for TOC removal.

4. Conclusions

The dielectric properties of the catalyst support play a crucial role on MW-assisted CWPO. With a MW absorber such as AC, formation of hot spots on the surface of the catalyst enhances the oxidative breakdown of the target pollutants. In this particular case, phenol mineralization upon CWPO was significantly improved under MW-radiation with the Fe/AC catalyst. The efficiency of H₂O₂ consumption was also improved and the highly toxic aromatic intermediates were barely detected and completely removed at around 15 min reaction time, working at 120 °C with 100 mg·L⁻¹ catalyst and the stoichiometric dose of H₂O₂ (500 mg·L⁻¹ for the 100 mg·L⁻¹ phenol solution). The formation of oligomeric condensation byproducts was also reduced with respect to the non-assisted process, and their presence in the liquid phase became almost negligible after 30 min reaction time.

In contrast, γ-Al₂O₃, being essentially transparent to MW radiation, did not show any significant enhancing effect in the MW-assisted process and even a lower efficiency of the Fe/γ-Al₂O₃ catalyst was observed compared to the non-assisted CWPO. This can be due to a higher formation of CBP covering active Fe sites.

Acknowledgements

This study is funded by the Spanish MINECO through projects CTQ2013-41963-R and CTM2016-76454-R. A.L. Garcia-Costa would like to thank the Spanish MINECO and the European Social Fund for their support through the PhD. grant BES-2014-067598.

Appendix A. Supplementary data

Supplementary data associated with this article can be found, in the online version, at <http://dx.doi.org/10.1016/j.apcatb.2017.06.058>.

References

- [1] C.M. Dominguez, P. Ocon, A. Quintanilla, J.A. Casas, J.J. Rodriguez, *Appl. Catal. B-Environ.* 144 (2014) 599–606.
- [2] J.A. Zazo, J.A. Casas, A.F. Mohedano, J.J. Rodriguez, *Appl. Catal. B-Environ.* 65 (2006) 261–268.
- [3] H.S. Park, J.R. Koduru, K.H. Choo, B. Lee, *J. Hazard. Mater.* 286 (2015) 315–324.
- [4] S.A. Messele, O. Soares, J.J.M. Orfao, F. Stuber, C. Bengoa, A. Fortuny, A. Fabregat, J. Font, *Appl. Catal. B-Environ.* 154 (2014) 329–338.
- [5] A. Rey, A.B. Hungria, C.J. Duran-Valle, M. Faraldo, A. Bahamonde, J.A. Casas, J.J. Rodriguez, *Appl. Catal. B-Environ.* 181 (1) (2016) 249–259.
- [6] F. Duarte, F.J. Maldonado-Hodar, L.M. Madeira, *Appl. Catal. B-Environ.* 129 (2013) 264–272.
- [7] F. Duarte, V. Morais, F.J. Maldonado-Hodar, L.M. Madeira, *Chem. Eng. J.* 232 (2013) 34–41.
- [8] P. Bautista, A.F. Mohedano, J.A. Casas, J.A. Zazo, J.J. Rodriguez, *Water Sci. Tech.* 61 (2010) 1631–1636.
- [9] P. Bautista, A.F. Mohedano, N. Menendez, J.A. Casas, J.J. Rodriguez, *Catal. Today* 151 (2010) 148–152.
- [10] M. Munoz, Z.M. de Pedro, J.A. Casas, J.J. Rodriguez, *Water Res.* 47 (2013) 3070–3080.
- [11] M. Munoz, Z.M. de Pedro, N. Menendez, J.A. Casas, J.J. Rodriguez, *Appl. Catal. B-Environ.* 136 (2013) 218–224.
- [12] R.S. Ribeiro, A.M.T. Silva, J.L. Figueiredo, J.L. Faria, H.T. Gomes, *Appl. Catal. B-Environ.* 140 (2013) 356–362.
- [13] F. Martinez, I. Pariente, C. Brebou, R. Molina, J.A. Melero, D. Bremner, D. Mantzavinos, *J. Chem. Technol. Biotechnol.* 89 (2014) 1182–1188.
- [14] F. Lucking, H. Koser, M. Jank, A. Ritter, *Water Res.* 32 (1998) 2607–2614.
- [15] C.M. Dominguez, P. Ocon, A. Quintanilla, J.A. Casas, J.J. Rodriguez, *Appl. Catal. B-Environ.* 140 (2013) 663–670.
- [16] N. Remya, J.-G. Lin, *Chem. Eng. J.* 166 (2011) 797–813.
- [17] N. Wang, P. Wang, *Chem. Eng. J.* 283 (2016) 193–214.
- [18] W.H. Sutton, *Am. Ceram. Soc. Bull.* 68 (1989) 376–386.
- [19] O.P.N. Calla, S.K. Mishra, D. Bohra, N. Khandelwal, P. Kalla, C. Sharma, N. Gathania, N. Bohra, S. Shukla, *Indian J. Pure Appl. Phys.* 46 (2008) 134–138.

[20] N. Li, P. Wang, C. Zuo, H.L. Cao, Q.S. Liu, *Environ. Eng. Sci.* 27 (2010) 271–280.

[21] E.A. Dawson, G.M.B. Parkes, P.A. Barnes, G. Bond, R. Mao, *Carbon* 46 (2008) 220–228.

[22] X.F. Zhang, J.W. Wang, Z.J. Yu, R.S. Wang, H.M. Xie, *Mater. Lett.* 63 (2009) 2523–2525.

[23] H. Lin, H. Zhu, H. Guo, L. Yu, *Mater. Lett.* 61 (2007) 3547–3550.

[24] S.J. Penn, N.M. Alford, A. Templeton, X.R. Wang, M.S. Xu, M. Reece, K. Schrapel, *J. Am. Ceram. Soc.* 80 (1997) 1885–1888.

[25] R. Vila, M. Gonzalez, J. Molla, A. Ibarra, *J. Nucl. Mater.* 253 (1998) 141–148.

[26] P. Yan, D. Bai, in: Z. Liu, X. Dong, Z. Liu, Q. Liu (Eds.) *Environ. Prot. Res. Expl. (Pts 1–3)* (2013) 1384–1387.

[27] L.B.G.P. Yan, W.T. Li, *Appl. Mech. Mat.* 448–453 (2014) 834–837.

[28] B.H. Jiang, Y. Zhao, Y. Jin, X.M. Hu, L. Jiang, X.M. Li, in: R. Chen, W.P. Sung (Eds.) *Biotech. Chem. Mat. Eng. (Pts 1–3)* (2012) 1443–1446.

[29] W. Pan, G. Zhang, T. Zheng, P. Wang, *RSC Adv.* 5 (2015) 27043–27051.

[30] A.Y. Atta, B.Y. Jibril, T.K. Al-Waheibi, Y.M. Al-Waheibi, *Catal. Comm.* 26 (2012) 112–116.

[31] G.H. Zhao, B.Y. Lv, Y. Jin, D.M. Li, *Water Environ. Res.* 82 (2010) 120–127.

[32] D.Y. Xu, Y.S. Zhang, F. Cheng, P. Dai, *J. Taiwan Inst. Chem. Eng.* 60 (2016) 376–382.

[33] X.D. Qi, Z.H. Li, *Pol. J. Environ. Stud.* 25 (2016) 1205–1214.

[34] Z. Ding, W.S. Guan, *J. Test. Eval.* 41 (2013) 693–700.

[35] A. Santos, P. Yustos, A. Quintanilla, G. Ruiz, F. Garcia-Ochoa, *Appl. Catal. B-Environ.* 61 (2005) 323–333.

[36] J.A. Zazo, A.F. Fraile, A. Rey, A. Bahamonde, J.A. Casas, J.J. Rodriguez, *Catal. Today* 143 (2009) 341–346.

[37] G.M. Eisenberg, *Ind. Eng. Chem.-Anal.* (1943) 327–328, Edition 15.

[38] J.A. Zazo, G. Pliego, S. Blasco, J.A. Casas, J.J. Rodriguez, *Ind. Eng. Chem. Res.* 50 (2011) 866–870.

[39] J.A. Menéndez, A. Arenillas, B. Fidalgo, Y. Fernández, L. Zubizarreta, E.G. Calvo, J.M. Bermúdez, *Fuel Process. Technol.* 91 (2010) 1–8.

[40] Z.H. Zhang, Y. Xu, M.L. Shen, D.D. Dionysiou, D. Wu, Z.L. Chen, F.Y. Li, D.N. Liu, F.Q. Zhang, *Environ. Prog. Sustain. Energy* 32 (2013) 181–186.

[41] J.A. Zazo, J.A. Casas, A.F. Mohedano, M.A. Gilarranz, J.J. Rodriguez, *Environ. Sci. Tech.* 39 (2005) 9295–9302.

[42] J.L.D. de Tuesta, A. Quintanilla, J.A. Casas, J.J. Rodriguez, *Appl. Catal. B-Environ.* 209 (2017) 701–710.

[43] M.E. Suarez-Ojeda, F. Stuber, A. Fortuny, A. Fabregat, J. Carrera, J. Font, *Appl. Catal. B-Environ.* 58 (2005) 105–114.